Research on improving low frequency oscillation characteristics of wind power system with DFIG-PSS-VI

Ping He[1,a], Mingming Zheng[1,b], Zhao Li[1], Qiyuan Fang[1], Xiaopeng Wu[1]

[1]College of Electric and Information Engineering Zhengzhou University of Light Industry, Zhengzhou, Henan, China

Abstract. The new energy represented by strong random wind power connecting to the power system may make the problem of inter-area low-frequency oscillation more serious. In this paper, a DFIG-PSS controller based on virtual impedance is constructed to solve the low-frequency oscillation problem in the wind power system. The step response of PSS-VI was carried out to test the effect of the controller to verify the advantages of PSS-VI than traditional PSS. The input signal of PSS-VI which is a controller based on PSS installed virtual impedance is the active power of DFIG. The output signal of PSS-VI is added to the reactive power control loop of rotor side controller of DFIG. DFIG-PSS-VI was built in Digsilent/Powerfactory software, and the simulation was carried out on the system of 4 machines and 2 regions. It is verified that PSS-VI can improve the low-frequency oscillation of wind power system.

1 Introduction

The new energy represented by strong random wind power connecting to the power system may make the problem of inter-area low-frequency oscillation more serious which affects the safe and stable operation of the power system [1]. Conventional synchronous generators use power system stabilizers (PSS) to provide additional damping during system disturbances and improve system low-frequency oscillation characteristics [2-3]. With the increase of wind power permeability, the power system requires wind turbines to provide damping, so it is very important to research additional damping control strategies similar to traditional synchronous generators.

It is illustrated that the influence of DFIG on the small signal stability in [4]. Reference [5] proposed the fast active power control technology of variable speed wind turbine, and applied these strategies to the frequency regulation and oscillation damping of the system. Reference [6] clarifies that adding appropriate PSS to doubly-fed induction generator (DFIG) can significantly enhance the contribution of wind farms to system damping. But this paper doesn't consider the influence of PSS on the system. The active power regulation of DFIG is carried out in [7], while the reactive power regulation of DFIG is carried out in [8]. It is pointed out in [9] that the active power regulation is easy to produce shafting oscillation. So it is best to adopt reactive power regulation of DFIG. It is studied that position and input signal of DFIG-PSS and controller parameters optimization in [10].

Under this background, this paper puts forward DFIG-PSS controller strategy based on virtual impedance (VI) [11] method to improve the wind power system low frequency oscillation characteristics. The DFIG-PSS-VI adds a virtual impedance block on the basis of the traditional PSS, and adopts the closed-loop negative feedback control mode to enhance the anti-interference ability of the controller. The rationality of the DFIG-PSS-VI is verified by the step response test of the controller. The output signal of the controller is added to the reactive power control block of the DFIG rotor side converter (RSC). Finally, the DFIG-PSS-VI model was built in the simulation software Digsilent/Powerfactory, and the simulation verification was carried out on the 4-machine 2-region system.

2 PSS Controller Based on Virtual Impedance

2.1 Traditional PSS

PSS is an auxiliary controller widely used in excitation control. By providing auxiliary control signals to the excitation system, the generator generates an electromagnetic torque component in the same phase as the rotor's electric angular velocity deviation, thus increasing the system damping and restraining the low-frequency oscillation of the power system. The transfer function is,

$$G(s) = K_{PSS}\frac{sT_W(1+sT_2)(1+sT_4)}{(1+sT_W)(1+sT_2)(1+sT_4)} \quad (1)$$

where, T_w is the time constant of the straight block, T_1, T_2, T_3 and T_4 are the time constants of the lead and lag blocks, and K_{PSS} is the gain of PSS.

*Corresponding author: [a]hplkz@126.com
[b]314764631@qq.com

2.2 Power System Stabilizer Based on Virtual Impedance Control

Virtual impedance is a control method that introduces virtual impedance loop in the control block to simulate the effect of actual line impedance [12-13]. The realization method of virtual impedance is more flexible. When the output impedance of the controller or line impedance is small, virtual impedance can be introduced to compensate. The virtual impedance method can be implemented in two ways including the virtual impedance designed based on the controller parameters and virtual impedance based on voltage control.

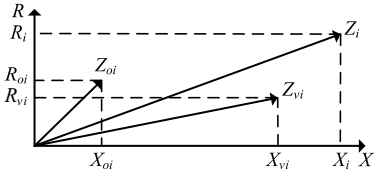

Fig.1 Vector diagram representation of virtual impedance

Based on the two methods, this paper selects a reasonable virtual impedance Z_{vi} to form a new output impedance Z_i with the output impedance Z_{oi} of PSS, and then changes the character of the system impedance to achieve the purpose of improving the stability of the system. It can be seen from Fig. 1 that the phase angle of Z_i can be changed when Z_{vi} is changed, and the output impedance of PSS-VI can be adjusted by changing the virtual impedance modulus value whose goal is to change the output signal of the controller, so as to ensure a good unit step response of the controller. The implementation of PSS-VI is shown in Fig. 2.

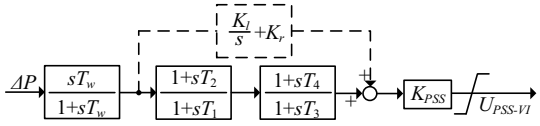

Fig.2 PSS-VI

The input signal of PSS-VI has a great impact on the controller performance, the input signal can be selected rotor speed, voltage, current and frequency. Based on residual analysis is the most common signal selection method. In this paper, the difference between the reference value Ps* and the measured value Ps of active power of DFIG is selected as the input signal of PSS-VI, and UPSS is the output signal of PSS-VI. Equation (2) is the transfer function of PSS-VI.

$$G_1(s)=K_{PSS}\frac{T_W}{1+sT_W}\left(\frac{(1+sT_1)(1+sT_3)}{(1+sT_2)(1+sT_4)}+K_r+\frac{K_I}{s}\right) \quad (2)$$

where, K_I and K_r are parameters of virtual impedance block, and K_{PSS} is the gain of PSS-VI. The equivalent circuit diagram of PSS after adding the virtual impedance is shown in Fig. 3.

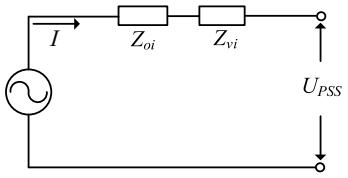

Fig.3 Equivalent Circuit Diagram of PSS-VI

The output signal of the controller can be obtained from equation (1) and (2),

$$\begin{cases} U_{PSS-VI}=\Delta PK_{PSS}\dfrac{T_W}{1+sT_W}\left(\dfrac{(1+sT_1)(1+sT_3)}{(1+sT_2)(1+sT_4)}+K_r+\dfrac{K_I}{s}\right) \\ U_{PSS}=\Delta PK_{PSS}\dfrac{sT_W(1+sT_2)(1+sT_4)}{(1+sT_W)(1+sT_2)(1+sT_4)} \end{cases} \quad (3)$$

In this paper, I is defined as the equivalent current of the controller, where Z_{oi} is defined as the equivalent output impedance of the controller and Z_{vi} is defined as the equivalent virtual impedance.

$$\begin{cases} U_{PSS-VI}=IZ_{oi}+IZ_{vi} \\ U_{PSS}=IZ_{oi} \end{cases} \quad (4)$$

where, $I=\Delta PK_{PSS}\dfrac{T_W}{1+sT_W}$, $Z_{oi}=\dfrac{(1+sT_1)(1+sT_3)}{(1+sT_2)(1+sT_4)}$, $Z_{vi}=K_r+\dfrac{K_I}{s}$.

It can be seen that the output signal of the controller can be changed by changing the parameters of the virtual impedance block, which is consistent with the above analysis.

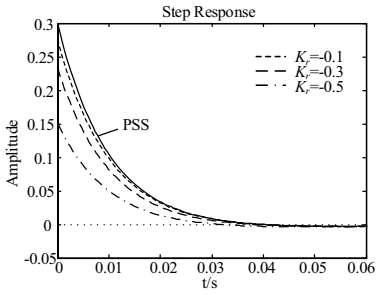

Fig.4 Step response curve of PSS-VI

As shown in Fig.4, the unit step response of PSS-VI has a faster response time than PSS, and the ideal unit step response of the controller can be obtained by changing the parameter K_r of the virtual impedance block.

3 DFIG-PSS Control Based on Virtual Impedance

The doubly fed induction generator adopts vector control strategy [14-15] to realize decoupling control of active power and reactive power, and considers maximum wind power and reactive power compensation, as shown in Fig. 5. This control strategy adopts traditional nested loop structure, which contains active power and reactive

power control loop and internal rotor current control loop in d-q frame. The reference current of rotor in d-q frame can be estimated effectively from the actual reference value and reactive power reference value, therefor the power loop controller with nested control structure is omitted.

The damping of DFIG with basic power and voltage control loops on the electromechanical oscillation mode of the power system is small, but the damping can be significantly enhanced through additional damping control. Through automatic voltage regulator (AVR), the signal of additional damping control is added to the active power control loop or reactive power control loop of DFIG.

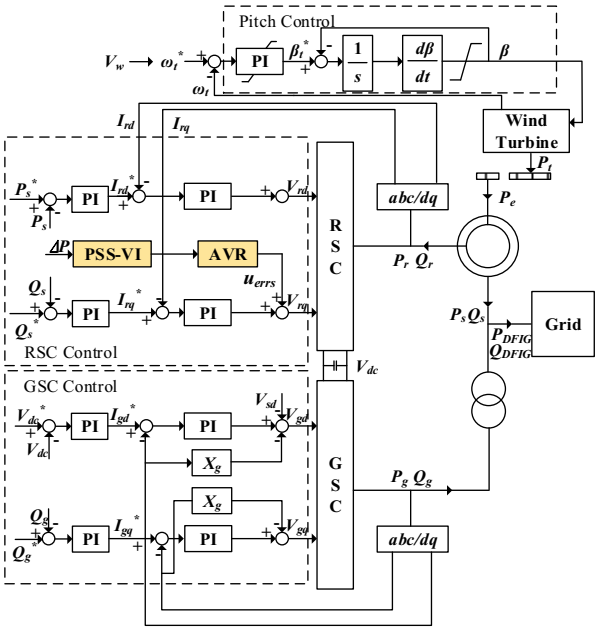

Fig.5 Control configuration of DFIG-PSS-VI

Active power regulation adjusts electromagnetic torque of generator more effective than reactive power regulation. Active power regulation makes shaft dynamic characteristics of DFIG worse, however, reactive power regulation could make the dynamic characteristics of the stator voltage worse. It is necessary to sacrifice part of the dynamic characteristics of DFIG for damping control, however it is necessary take damping control and system dynamic performance into account in the actual implementation at the same time. In this paper, the output control signal UPSS-VI of PSS-VI is added into the reactive power control loop, where the quadrature component of rotor voltage is obtained by summing. After PSS-VI controller is added, the relationship between rotor current and RSC output voltage can be obtained from equation (5).

$$\begin{cases} V_{rd} = [(P_s^* - P_s)(K_{p1} + \dfrac{K_{i1}}{s}) - i_{rd}](K_{p3} + \dfrac{K_{i3}}{s}) \\ V_{rq} = [(Q_s^* - Q_s)(K_{q1} + \dfrac{K_{i2}}{s}) - i_{rq}](K_{p3} + \dfrac{K_{i3}}{s}) - u_{errs} \end{cases} \tag{5}$$

where, K_{p1}, K_{i1}, K_{p3}, K_{i3}, K_{q1} and K_{i2} are parameters of PI controller of the rotor-side converter. ω_s is the angular velocity of synchronous magnetic field rotation, uerrs is the output signal of PSS-VI through the AVR device, P_s is stator active power, Q_s is stator reactive power, P_s^* is the reference value of stator active power and Q_s^* is the reference value of stator reactive power.

$$u_{errs} = \frac{U_{PSS-VI} - \dfrac{u}{1+sT_r}}{sT_e + K + \dfrac{sK_{f1}}{sT_{f1}} \dfrac{1+sT_c}{1+sT_b} \dfrac{K_a}{1+sT_a}} \tag{6}$$

where, T_e, K_{f1}, T_c, T_b, T_{f1}, K_a, T_a and T_r are parameters of AVR, and u is the measured value of stator voltage.

According to the relationship between voltage, flux and current on the stator side, the stator current and power can be expressed as equation (7).

$$\begin{cases} P_s = u_{ds} i_{ds} = -\dfrac{U_s L_m}{L_s} i_{rd} \\ Q_s = u_{ds} i_{qs} = -\dfrac{U_s^2}{\omega_s L_s} - \dfrac{U_s L_m}{L_s} i_{rq} \end{cases} \tag{7}$$

where, L_m is mutual inductance of coaxial equivalent windings of stator and rotor in *d-q* frame, L_s is self-inductance of stator equivalent winding in *d-q* frame. The relationship between stator output power and PSS-VI parameters can be obtained.

$$Q_s = -\frac{u_s^2}{\omega_s L_r} - \frac{u_s L_m [V_{rd} - H(Q_s^* + \dfrac{u_s^2}{\omega_s L_r})]}{(H u_s L_m - L_r)} \frac{1}{D - u_{errs}} \tag{8}$$

4 Simulation Analysis

The DFIG-PSS-VI model was built in DIgsilent/PowerFactory software, and the results of simulation carried out on the 4-machine 2-area power system which is used to verify PSS-VI could improve the low frequency oscillation characteristics of power system with wind power. The reference capacity of the system is 100MVA whose frequency is 50Hz and the transmission power of the tie-line is 400MW. Region 1 and Region 2 of the system whose node 3 is the reference node are connected by double loop connection lines. G_1, G_2, G_3 and G_4 are 4 thermal power units with rated capacity of 900MVA and rated voltage of 20kV, whose output active power are 700MW. As shown in Fig. 6, DFIG access point is bus 10. The parameters of PSS-VI are as follows, $T_w = 0.01$, $T_1 = 0.08$, $T_2 = 0.4$, $T_3 = 0.3$, $T_4 = 0.06$, $K_{PSS} = 0.3$, $K_r = -0.9$ and $K_l = 0.51$.

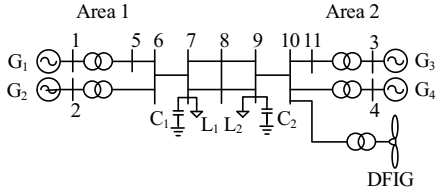

Fig.6 Two-area four-machine system with DFIG

Case 1: The power transmitted on the tie line from region 1 to region 2 is 300MW.

Case 2: The power transmitted on the tie line from region 1 to region 2 is 400MW.

Case 3: The power transmitted on the tie line from region 1 to region 2 is 600MW.

It is shown the variation of system oscillation modes under different operating modes with PSS or PSS-VI in Tab. 1. Mode 1 and 2 represent the local oscillation of the generator set in region 1 and 2, however Mode 3 and mode 4 represent the regional oscillation of the generator set between region 1 and 2. Mode 4 represents the new inter-regional oscillation mode after DFIG is connected to the system. According to Tab. 1, the damping improvement of DFIG-PSS is slightly better than the damping ratio improvement of DFIG-PSS-VI under different operation conditions for the oscillation mode 1. For the oscillation mode 3, with the increase of transmission power of the tie line, the damping improvement of the system with DFIG-PSS-VI is better than that with DFIG-PSS. For oscillation mode 4, DFIG-PSS-VI is better than DFIG-PSS in improving the system damping ratio under different operation conditions. However, with the increase of system tie line power, the improving effect of DFIG-PSS-VI on the system damping ratio is gradually weakened.

Tab.1 Electro-mechanical oscillatory modes with different controllers

Case	Mode	With PSS			With PSS-VI			SCG
		λ	f/Hz	ξ/%	λ	f/Hz	ξ/%	
1	1	-0.585±j6.402	1.019	9.101	-0.580±j6.400	1.018	9.028	G_1,G_2
	2	-0.671±j6.550	1.042	10.195	-0.617±j6.550	1.043	10.196	G_3,G_4
	3	-0.292±j3.276	0.521	8.888	-0.282±j3.295	0.525	8.528	G_1,G_2,G_3,G_4
	4	-0.605±j2.928	0.466	20.256	-1.343±j3.596	0.572	34.992	G_1,G_2,G_3,G_4,DFIG
2	1	-0.616±j6.389	1.017	9.601	-0.614±j6.389	1.017	9.526	G_1,G_2
	2	-0.651±j6.547	1.042	9.897	-0.651±j6.547	1.042	9.597	G_3,G_4
	3	-0.265±j3.165	0.504	8.331	-0.318±j3.156	0.502	10.046	G_1,G_2,G_3,G_4
	4	-0.619±j2.907	0.463	20.838	-1.124±j3.596	0.572	29.822	G_1,G_2,G_3,G_4,DFIG
3	1	-0.618±j6.502	1.035	9.466	-0.618±j6.502	1.035	9.467	G_1,G_2
	2	-0.699±j6.348	1.010	10.950	-0.693±j6.347	1.010	10.851	G_3,G_4
	3	-0.469±j2.843	0.452	16.279	-0.403±j2.359	0.376	16.838	G_1,G_2,G_3,G_4
	4	-0.512±j2.444	0.389	20.514	-1.001±j3.622	0.576	26.646	G_1,G_2,G_3,G_4,DFIG

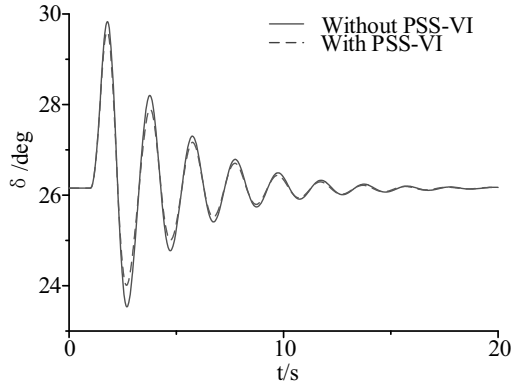

(a) fluctuation of load

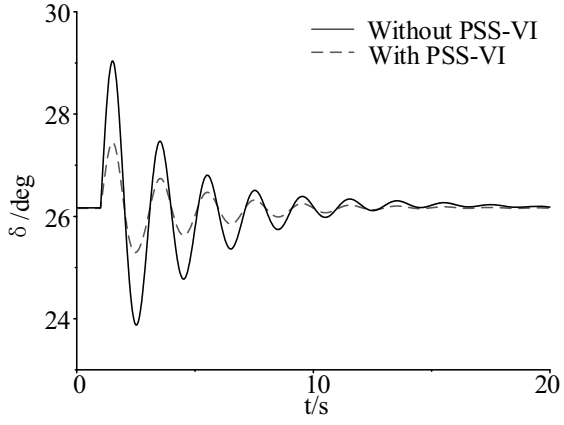

(b) three-phase short-circuit fault

Fig.7 Response curves of G_1

In order to verify the effectiveness of PSS-VI better, it is assumed that the active load of system whose transmission power of the tie line is 400MW will be set to step 10% at 1s and recover at 1.5s. The simulation time will be 20s. It is shown the relative power angle δ of generator G1 when load fluctuations occur in Fig. 7(a). A three-phase short-circuit fault occurs at one of the double-circuit lines of line7-8 at 1.0 s and then is cleared 100 ms later. Then it is in case 2 to gain the relative rotor angle curves between G1 and G3 which is shown in Fig. 8 (b). It is observed from Fig. 7 that the relative rotor angle is divergent in the case without PSS-VI installed, and the time of remaining stable is longer. The fluctuation range of these curves get decrease while the stable time is shorted significantly when the PSS-VI is respectively installed.

5 Conclusions

To solve the low-frequency oscillation problem of the wind power system, this paper constructed a DFIG-PSS controller based on virtual impedance which was built in DigSilent/Powerfactory simulation software. Taking the 4-machine 2-region system as an example, the constructed controller was installed into the reactive power control loop of the rotor-side controller of DFIG, and the improvement effect of the designed controller on the low-frequency oscillation characteristics of the system was verified by time domain simulation. The main conclusions are as follows:

(1) The virtual impedance controller whose step response characteristics is better than the traditional controller can improve the stability of the system more obviously

(2) PSS-VI installed in DFIG rotor-side reactive power control loop can improve the low-frequency oscillation of the wind power system, and it also has a certain effect when the power of the tie line changes.

(3) DFIG-PSS-VI have a certain influence on system damping whose improvement effect on intra-regional oscillation is limited. However, the controller provides a new idea for suppressing inter-regional low-frequency oscillation of regional interconnected systems with wind power.

Acknowledgement

This work is jointly supported by the National Natural Science Foundation of China (NSFC) (No. 51507157), the Scientific and Technological Research Foundation of Henan Province (No. 202102210305), and the Key Project of Zhengzhou University of Light Industry (2020ZDPY0204).

References

1. Y. Wang, J. H. Meng, X.Y. Zhang, L. Xu. Control of PMSG-based wind turbines for system inertial response and power oscillation damping. J. IEEE Transaction on Sustain Energy, 6, 2: 565-574 (2015).
2. K. M. Sreedivya, P. A. Jeyanthy and D. Devaraj. An Effective AVR-PSS Design for Electromechanical Oscillations Damping in Power System, In: 2019 IEEE International Conference on Clean Energy and Energy Efficient Electronics Circuit for Sustainable Development (INCCES). Krishnankoil. 1-5 (2019).
3. S. Y. Lu, W.Y. Zhang, T. Wang, Y. P. Cai, et al. Parameter Tuning and Simulation Analysis of PSS Function in Excitation System with Suppression of Low Frequency Oscillation, In: 2019 IEEE 8th International Conference on Advanced Power System Automation and Protection (APAP). Xi'an. 474-479 (2019).
4. J. L. Garcı, O. G. Bellmunta, F. D. Bianchi, A. Sumpera. Power oscillation damping supported by wind power: A review. J. Renewable and Sustainable Energy Reviews, 16, 7: 4982-4993 (2012).
5. Y. Liu, J. R. Gracia, T. J. King, Y. L. Liu. Frequency regulation and oscillation damping contributions of variable-speed wind generators in the U.S. Eastern Interconnection (EI). J. IEEE Transactions on Sustainable Energy, 6, 3: 951-957 (2015).
6. F. M. Hughes, O. A. Lara, N. Jenkins, G. Strbac. A power system stabilizer for DFIG-based wind generation. J. IEEE Transactions on Power Systems, 21, 2: 763-772 (2006).
7. M. Singh, A. J. Allen, E. Muljadi, V. Gevorgian, Y.C. Zhang, S. Santoso. Interarea oscillation damping controls for wind power plants. J. IEEE Transactions on Sustainable Energy, 6, 3: 967-975 (2015).
8. K. Liao, Z.Y. He, Y. Xu, C. Guo, Y. D. Zhao, K. P. Wong. A sliding mode based damping control of DFIG for interarea power oscillations. J. IEEE Transactions on Sustainable Energy, 8, 1: 258-267 (2017).
9. L. L. Fan, H. P. Yin, Z. X. Miao. On Active/Reactive Power Modulation of DFIG-Based Wind Generation for Interarea Oscillation Damping. J. IEEE Transactions on Energy Conversion, 26, 2:513-521 (2011).
10. X. Y. Bian, Y. Ding, Q. Y. Jia, L. Shi, X.P. Zhang, L. L. Kwok. Mitigation of sub-synchronous control interaction of a power system with DFIG-based wind farm under multi-operating points. J. IET Generation, Transmission & Distribution, 12, 21: 5834-5842 (2018).
11. X. Zhang, Q. Zhong and W. Ming. Stabilization of Cascaded DC/DC Converters via Adaptive Series-Virtual-Impedance Control of the Load Converter. J. IEEE Transactions on Power Electronics, 31, 9: 6057-6063 (2016).
12. M. D. Pham, H.H. Lee. Effective Coordinated Virtual Impedance Control for Accurate Power Sharing in Islanded Microgrid. J. IEEE Transactions on Industrial Electronics, 68, 3: 2279-2288 (2021).
13. H.Y. Li, T. Zheng, S.F. Huang, Y.P. Wang. UPFC fault ride-through strategy based on virtual impedance and current limiting reactor. J. International Journal of Electrical Power & Energy Systems, 125:1-13 (2021).
14. S. N. Gao, H.R. Zhao, Y.H. Gui, D. Zhou, F. Blaabjerg. An Improved Direct Power Control for Doubly Fed Induction Generator. J. IEEE Transactions on Power Electronics, 36, 4: 4672-4685 (2021).
15. C. Wu, D. Zhou, F. Blaabjerg. Direct Power Magnitude Control of DFIG-DC System Without Orientation Control. J. IEEE Transactions on Power Electronics, 68, 2: 1365-1373 (2021).